Proceedings of ASME Turbo Expo 2011
GT2011
June 6-10, 2011, Vancouver, British Columbia, Canada

GT2011-45125

STUDY ON THE OPERATIONAL WINDOW OF A SWIRL STABILIZED SYNGAS BURNER UNDER ATMOSPHERIC AND HIGH PRESSURE CONDITIONS

C. Mayer*, J. Sangl, T. Sattelmayer
Lehrstuhl für Thermodynamik, TU München
D-85748 Garching, Germany
E-mail: mayer@td.mw.tum.de

T. Lachaux, S. Bernero
Alstom Power
Baden, Switzerland

ABSTRACT

Providing better fuel flexibility for future gas turbine generations is a challenge as the fuel range is expected to become significantly wider (natural gas, syngas, etc.). The technical problem is to reach a wide operational window, regarding both operational safety and low emissions. In a previous paper an approach to meet these requirements has already been presented. However, in this previous study it was difficult to exactly quantify the improvement in operational safety due to the fact that the flashback phenomena observed were not fully understood. The present continuative paper is focused on a thorough investigation of operational safety also involving the influence of pressure on flashback and the emissions of the proposed burner concept. To gain better insight in the character of the propagation and to visualize the path of the flame during its upstream motion, tests were done on an atmospheric combustion test rig providing almost complete optical access to the mixing section as well as the flame tube. OH^* chemiliuminescence, HS-Mie scattering and ionization detectors were applied and undiluted H_2 was used as fuel for the detailed analysis . To elaborate the influence of pressure on the stability behavior additional tests were done on a pressurized test rig using a downscaled burner. OH^* chemiluminescence, flashback and lean blow out measurements were conducted in this campaign, using CH_4, CH_4/H_2 mixtures and pure H_2. The conducted experiments delivered the assets and drawbacks of the fuel injection strategy, where high axial fuel momentum was used to tune the flow field to achieve better flashback resistance.

*Address all correspondence to this author.

NOMENCLATURE

Symbols

C_b	Constant for Konle Model [s]
D	Diameter [m]
g	Wall Velocity Gradient [1/s]
I	Intensity [-]
$\dot{m}$	Mass Flow Rate [kg/s]
p	Pressure [bar]
Δp	Pressure Drop [%]
Re	Reynolds Number [-]
s_l	Laminar Flame Speed [m/s]
s_t	Turbulent Flame Speed [m/s]
t	Time [s]
T	Temperature [K]
$\overline{u}$	Axial Bulk Velocity [m/s]
u'	Velocity Fluctuation [m/s]
x	Axial Coordinate [m]
X	Volume Fraction (Fuel Air Mixture) [%]
η	Dynamic Viscosity [Pa s]
γ	Volume Fraction (Fuel Composition) [%]
ϕ	Equivalence Ratio [-]
ρ	Density [kg/m^3]

Indices

amb	Ambient
ax	Axial
Br	Burner
crit	Critical
exp	Experiment
max	Maximum

Abbreviations

CIVB	Combustion Induced Vortex Breakdown
HS	High Speed
LBO	Lean Blow Out
N	Nozzle
PIV	Particle Image Velocimetry
RCZ	Recirculation Zone
WBLF	Wall Boundary Layer Flashback

INTRODUCTION

The global shortage of resources and the threat of global warming forces the gas turbine industry to look for alternative fuels to be fired in stationary gas turbines of the next generation. Syngas, which can be derived from different primary fuels could be an approach to the problem. The main active components of these fuels are hydrogen (H_2) and carbon monoxide (CO) in different composition, depending on the primary fuel and gasification process. The challenge is to develop flexible combustion systems, which are able to cope with these syngases and their properties (varying composition, higher reactivity, lower volumetric heating value), but also burn natural gas, which is going to remain the most common fuel in premixed combustion applications. The quality criteria for evaluating burner designs are high resistance against instabilities and low emissions. Note that thermo acoustic instabilities are not addressed in this work.

The burner type used in this work is an aerodynamically stabilized swirl burner, which provides enough swirl for the proper stabilization of natural gas flames, which anchor at a bubble shaped recirculation zone (RCZ) generated downstream of the breakdown of the vortical flow. To meet the challenge of an instability resistant design also for highly reactive syngases the high fuel momentum, which is available when using syngas, is used to adapt the flow field to the needs of such reactive flames.

The paper is a continuation of the work presented in [1], which also contains a literature review. In this previous paper the basic approach of tailoring the flow using fuel momentum was presented. Aerodynamics and mixing studies were done in a water channel and also first atmospheric combustion experiments were presented, showing encouraging results concerning operational safety and mixing quality. Since the experiments reported in the previous study allowed no optical access to the mixing section, difficulties to exactly quantify the improvement of operational safety against combustion induced vortex breakdown (CIVB) and wall boundary layer flashback (WBLF), respectively, were encountered. The type of flashback occurring in these tests and in particular the interaction of CIVB and WBLF were not clearly understood.

To gain better insight in the character of the propagation and to visualize the path of the flame during its upstream motion, further tests were done in the modified atmospheric combustion test rig providing almost complete optical access to the mixing section as well as the flame tube. In this campaign, OH^*-chemiluminescence videos with sufficient temporal resolution for the tracking of the flame during upstream propagation were recorded, high-speed Mie scattering was employed, delivering planar information of the flame front position on the basis of the drop of the seeding particle density over the flame front and ionization detectors were used to characterize flame propagation along the wall. In these tests several injection methods already presented in the previous paper [1] were employed to quantify their influence on operational safety and NO_x-emissions. The influence of a diffuser attached to the burner exit on the operational window was additionally investigated. Interestingly, in these tests the three different flashback phenomena were observed in the same small operational range, CIVB, flashback against the bulk flow and WBLF.

For further information on the operational window of the burner additional combustion tests under elevated pressure with a downscaled burner were conducted at a limited number of operating conditions. Again, the performance of different injection methods was tested for a wide range of fuel reactivity. OH^* chemiluminescence measurements of the flame in the combustion chamber as well as flashback and lean blow out (LBO) measurements resulting in stability maps showed the influence of pressure on burner performance.

In all experiments addressing the fuel injection concept undiluted H_2 was used, whereas in the pressurized tests also undiluted CH_4/H_2 mixtures were employed. As the consequence of testing without diluents the tests represent the worst case scenario for burner operation. In particular, the beneficial effects of the high available fuel momentum and lower reactivity of diluted MBTU and LBTU syngas were not employed in the tests. The study reported in [1] showed already that the potential of syngas regarding stability and emissions is much better compared to hydrogen used in the tests presented in the paper. The influence of dilution on the potential of the concepts presented below has not yet been studied.

BURNER GEOMETRY & FUEL INJECTION CONCEPT

Below, only a short description of the burner and injection concept is given, as more detailed information has already been published in [1]. The burner consists of a thick walled hollow cone comprising four tangential slots, which are symmetrically arranged around the circumference and end tangentially in the inner cone surface.

As sketched in Figure 1 the air flow (light blue arrows) enters the burner through the tangential slots, creating a swirling flow in the burner, and unswirled through the annular open gap at the apex of the cone. Two types of fuel injectors are employed: The fuel is axially injected at the apex of the burner and/or through rows of injector holes placed along the four trailing edges (TE) formed by the inner walls of the swirler slots and the inner cone

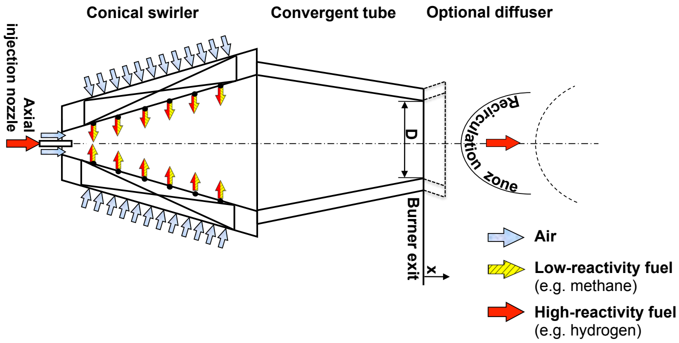

FIG. 1: Burner geometry and injection strategy

surface. The TE-injection is supposed to achieve good mixing quality and emissions, with minimum effect on the flow field. In contrast, the axial injection intends to use the fuel momentum to influence the position of RCZ as indicated by the red arrow and shown in [1]. By axial fuel injection with high velocities the total pressure on the axis is increased and the swirl number drops. These modifications of the flow field are supposed to generate a more suitable aerodynamics for flame stabilization of highly reactive fuels. Downstream of the swirler, the air fuel mixture passes the convergent mixing section and optionally a diffuser before being burned in the combustion chamber.

TEST RIGS AND EXPERIMENTAL PROCEDURES

Atmospheric combustion test rig

Combustion experiments were made using an atmospheric combustion test rig with 400 kW thermal power. The test rig [2] [3] consists of an air supply system, where the air coming from a compressor can be preheated to 500°C max., and a flexible fuel supply system (Figure 2). One option is to mix air and fuel upstream of the burner, the so-called externally premixed configuration (1). The second option is the fuel injection into the burner head (2a: injection at the cone apex; 2b: injection along the slots). The atmospheric experiments subsequently presented were made with undiluted hydrogen and the preheat temperature was 400°C.

The air cooled mixing tube and the cylindrical combustion chamber are both made of silica fused glass, which allows full optical access to the flame zone also during flashback. The burned gas then enters a water-cooled chamber, which is isolated with ceramics. Far downstream of this second chamber the exhaust is sampled in the middle using a suction probe.

The measurement systems used here were an HS-ICCD camera, a HS-PIV system, ionization detectors and standard exhaust gas analysers [1]. The camera used was an Ultima APX I^2 Fastcam from Photron with an UV bandpass filter for the OH^* chemiluminescence signal. It was placed perpendic-

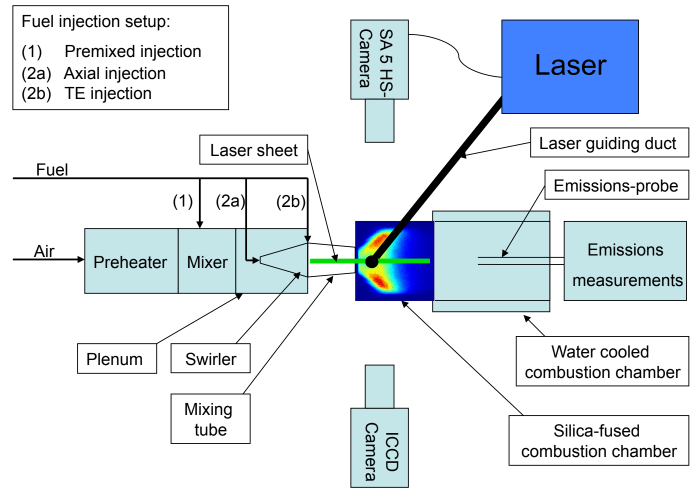

FIG. 2: Scheme of the atmospheric combustion test rig

ular to the combustion chamber (see Figure 2). The Abel-deconvolution algorithm proposed in [4] was used to extract planar information from the averaged, line of sight integrated OH^*-chemiluminescence images. The HS-PIV experiments were done with a SA5 Photron HS-Camera, which was coupled with a New Wave Pegasus Nd:Ylf Laser. The seeding particles (TiO_2) were introduced between the preheater and the mixer.

High pressure combustion test rig

Information on the effect of pressure on the flame shape and on the operational window of the burner was gained from additional combustion tests under elevated pressure using a down-scaled burner (factor 2.3) without TE-injectors. For this purpose, OH^*-chemiluminescence of the flame in the combustion chamber and stability limits (flashback and LBO) were measured. Figure 3 gives an overview of the high pressure test rig, which is described in detail in [5] and [6].

The combustion air enters an electrical air preheater, which is connected to a supply tube. For the externally premixed setup with perfect fuel-air mixing, the fuel gas is injected at the entry

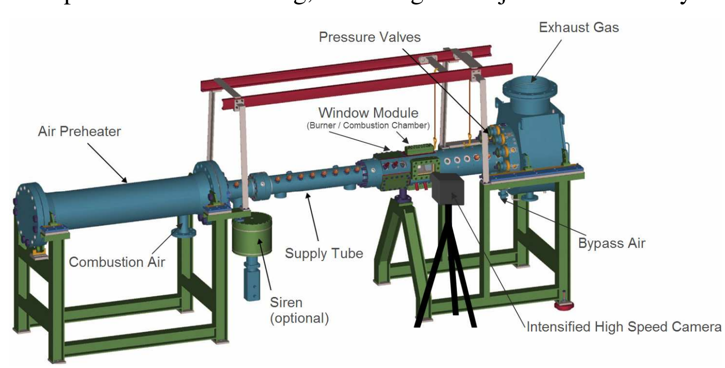

FIG. 3: High pressure test rig

of this supply tube. The water cooled window module represents the core of the test rig. The burner including the diffuser is mounted in the upstream part and the flame is stabilized in the downstream section. Rectangular access ports allow observation of the flame through quartz glass windows. The overlapping arrangement of the large windows allows an undisturbed observation of more than one half (approx. 65%) of the flame through each window on both sides. The valve support disk forms the last module which guides the exhaust gases radially outwards to 9 pressure valves at the circumference, where the gas is expanded before it flows to the stack.

For measurement of the OH^* chemiluminescence the same camera as for the atmospheric tests was used. The camera was mounted normal to the burner axis and downstream of the burner exit and observed the flame through one of the side windows of the window module (Figure 3). A frame rate of 1000fps and camera resolution of 1024×512 pixels, which is equal to a field of view of $5\ D \times 2.5\ D$ was used. Due to the axial symmetry of the flame only one half of the flame was analyzed. The images were averaged before Abel deconvolution [4] was employed.

Experimental procedures

On both test rigs similar experimental procedures were applied. Starting with a stable pre-selected operating point, the combustion air flow of a stable operating point was kept constant while the equivalence ratio (Φ) was ramped up and down for flashback and lean blow out measurements, respectively. The flashback limit was defined by a steep temperature increase monitored with thermocouples close to the swirler. As soon as the flame started to oscillate forwards and backwards from a stable position at the burner exit to an undefined position downstream of the burner exit, the measurement was stopped and the corresponding operation point was defined as LBO.

RESULTS AND DISCUSSION

Atmospheric combustion experiments

Flashback characterization in externally premixed mode: As shown in [1] the characterization of the flashback types, occurring when driving the test rig towards operating points far from machine conditions, is essential for the optimization of the burner against flashback, because countermeasures against WBLF and CIVB are essentially different. All experiments reported in this section were done at a bulk velocity of air at the burner outlet of $\bar{u} \approx 21$m/s and in externally premixed configuration to exclude fuel injection effects. These are presented in the next section. Experiments at higher and lower mass flows were also conducted and showed analogue results, why they are not shown here.

First the **configuration with diffuser** mounted at the mixing tube end was investigated. All employed measurement techniques consistently indicate that the type of flashback occurring in this configuration is WBLF. Interestingly, a change of flame stabilization pattern can be observed before flashback takes place for this configuration. The OH^*-chemiluminescence images in Figure 4 show this transition at 1 kHz sampling frequency. One

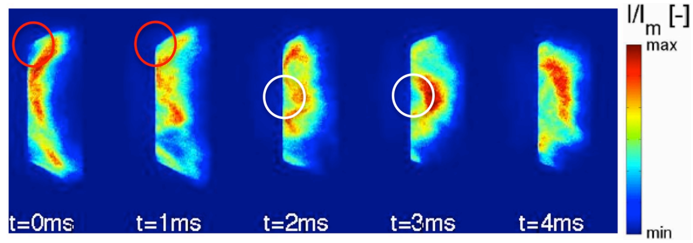

FIG. 4: Change of stabilization pattern with diffuser

can see that the flame changes its stabilization pattern from a flame anchored in the inner RCZ exhibiting tendencies to periodically ignite in the outer shear layer (t=0ms) to a flame stabilizing completely in the outer shear layer. Figure 5 gives a schematic of

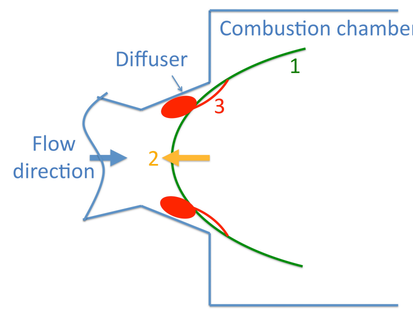

FIG. 5: Transition of flame stabilization pattern

how this changeover takes place. The transition is initiated when the RCZ (1) moves upstream due to the increase of equivalence ratio (2). Suddenly, the flame stabilizes near the wall of the diffuser. This effect can be seen when looking at the red circles in Figure 4, where at t=0ms the flame has not yet stabilized at the diffuser wall and at t=1ms the flame has moved into the diffuser. As the consequence of this flame propagation into the diffuser the fuel air mixture is accelerated on the axis and the RCZ is pushed downstream. The downward shift of the flame on the axis can also be seen in Figure 4 (white circles).

From the line of sight integrated chemiluminescence images it is concluded that after this change of the stabilization pattern the flame root is located in the outer shear layer and that this mode is qualitatively similar to the situation observed on tube burners without swirl (3), which typically exhibit WBLF. Before WBLF occurs in the swirl burner with diffuser the flame ignites close to the walls of the mixing tube outlet and by further increase in equivalence ratio, the flame starts propagating upstream

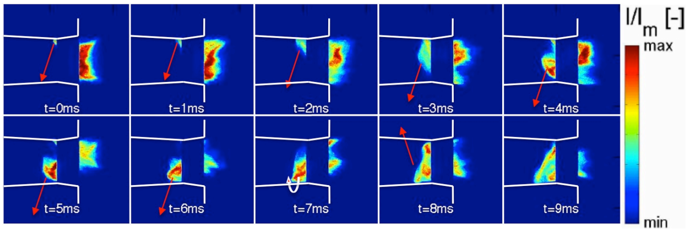

FIG. 6: Wall boundary layer flashback with diffuser

along the wall. Figure 6 shows the first phase of WBLF taking place in the mixing tube. Watching the videos one can clearly see that the flame moves in along the wall and rotates around the burner axis. The red arrows show the direction the flame moves. While propagating upstream, the flame tip rotates from the top downward along the back side of the tube and at t=7ms it moves up again along the front side. The sense of rotation observed indicates that this effect results from the rotation of the air fuel mixture in the mixing tube. The rotation continues until the flame has arrived in the swirler.

Flashback for the configuration with diffuser was investigated for different mass flows and the process was always the same; the sole parameter that changes is the velocity of the flame propagation during flashback, which depends on the equivalence ratio when flashback occurs.

Since the OH*-images are line of sight integrated, the three dimensional flame propagation along the wall is not unambiguously visible. To address this issue the silica fused mixing tube was replaced by a stainless steel tube with 24 ionization detectors. Their working principle is explained in [7]. These sensors react on the ionization during combustion and are used here to detect the hydrogen flame at the wall during WBLF. The sensors and the electronics are in-house developments. The sensors were mounted in four rows with six equally distributed sensors around the circumference in each row. The first row was placed at x=-0.2 D upstream of the mixing tube exit. The four rows have a distance of 0.44 D from each other and are placed in upstream direction relative to the mixing tube outlet. The sampling frequency was 10 kHz.

Figure 7 shows the detected signal of the first row being the closest to the mixing tube exit during flashback. The measured signal indicates clearly that the flashback type here is WBLF. The flame enters the mixing section very close to sensor 2, which is the first sensor to detect the flame. Then the flame rotates to the sensors one, six, five and four. Except of sensor 1, which showed lower response due to manufacturing tolerances, all sensors also show that the flame rotates, while it propagates upstream. The signal increases from sensor to sensor, which is due to the higher ionization intensity, when the flame gets thicker at the sensor due to the upstream propagation. The following sensor rows 2 to 4 confirm the rotating propagation of the flame along the wall (not shown here).

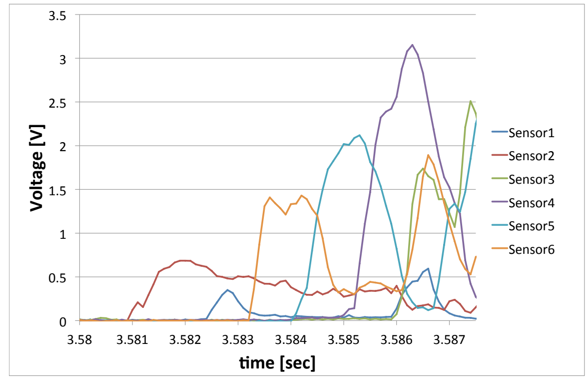

FIG. 7: WBLF detection with ionization detectors (row 1)

After observing for the burner with diffuser the flow transition with anchoring of the flame near the diffuser walls precedes WBLF the study was extended to the **configuration without diffuser**. The appearance of flashback occurring in this configuration is shown in the following pictures. Interestingly, a sequence of three flame propagation phenomena was observed during flashback for this configuration. In the first phase from

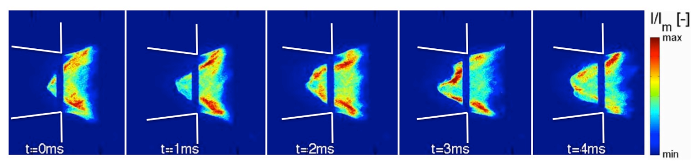

FIG. 8: Initial phase of flame flashback

time step 0ms until 4ms the flame first penetrates the end of the mixing tube in the center of the swirling flow. During this phase the flame has a conical shape as shown in Figure 8. The flame propagation corresponds to the pattern earlier observed for CIVB driven flashback [2] [3]. Then, the flame stays in this position until t=17ms. The flame changes to an almost half spherical shape, before propagating further upstream, as seen in Figure 9. From t=20ms to t=24ms the flame oscillates between the conical and half spherical shape. This indicates that the further flame propagation through the center is stopped and that flame propagation is fast enough to reach the wall region. The latter can be attributed to the turbulent flame speed, which reaches the magnitude of the flow speed upstream of the flame region (see green curve in Figure 14), because the experiments were run at a small fraction of velocities typical for engine operation. However, the videos indicate that the transport of reaction towards the flame is of stochastic nature and governed by large vortices present in the swirling flow. At t=24ms the reaction zone approaches the wall (red circle), but until t=26.5ms the velocity gradients at this location seem to be still too high for further flame propagation along the wall. Finally, after the flame shape has become flat enough, the reaction zone gets contact to the wall further upstream, where the velocity gradient is too small to prevent WBLF due to the low

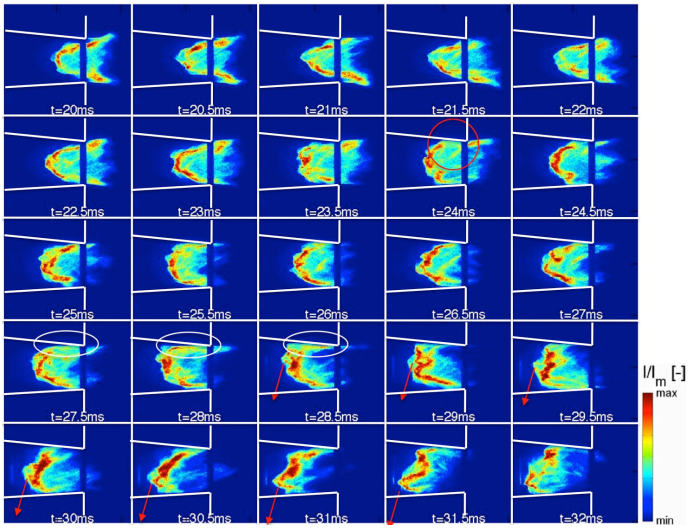

FIG. 9: Transitional phase of flame flashback

flow rate in the experiment. It can be concluded that the observed transition is closely linked to the conical shape of the mixing tube with increasing velocity gradients in streamwise direction. This increase was quantitatively investigated in water channel experiments. The velocity gradient increases by a factor of approx. 2 from the mixing tube inlet to the outlet. From t=27.5ms until t=28.5ms one can see the flame propagating along the top of the mixing tube (white ellipse). Then, from here the flame rotates along the mixing tube wall until it reaches the swirler (red arrows) as seen before in the section where the configuration with diffuser was discussed.

The observations clearly indicate that the flashback observed for this burner configuration has three consecutive phases staring with an upwards shift of the flame typical for CIVB driven flashback, followed by flame propagation through the bulk flow from the center of the flow towards the mixing tube wall driven by large vortices and ending with WBLF once the reaction zone touches the wall in a region, where the wall velocity gradient is too small to prevent flame propagation along the wall. At higher burner pressure drops typical for gas turbine operation the first phase does not occur and as the consequence flashback cannot be provoked even for $\phi = 1$.

Since the chemiluminescence image sequences are line of sight integrated and lack true local information, additional HS-Mie scattering measurements were done during flashback, where planar information on the flame propagation in the laser sheet (green line in Figure 2) was acquired. Since these measurements fully confirmed all observations made above and did not provide any additional insight, they are not shown here.

Influence of fuel injection: The investigations of the externally premixed **configuration without diffuser** were extended to tests with fuel injection in the swirler to address the question to what extend flashback can be avoided by using axial fuel momentum when injecting undiluted hydrogen. In the further study a combination of the TE injection and axial injection at the apex of the conical swirler was investigated.

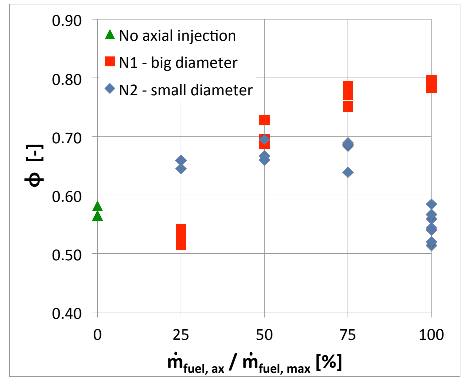

FIG. 10: Flashback characteristic for different ratios between axial and TE-injection using different nozzles (N1, N2)

In a first step the flashback characteristics for different injection ratios of axial injection and TE-injection was investigated (Figure 10). Here, two fuel nozzles, one with big diameter (N1, low momentum) and one with small diameter (N2, high momentum) were investigated. The bulk velocity of the air at the burner outlet was $\bar{u} \approx 21$m/s in these tests. As expected, the flashback characteristic of the burner improved considerably when using the axial injection properly. For the interpretation of these results one should have in mind that two effects have to be considered, which overlay one another: Based on the selected fuel split the momentum increase on the axis as well as the radial fuel profile at the burner exit are simultaneously influenced.

The fuel split with 25% axial injection for the fuel nozzle N1 shows this clearly. The momentum on the axis is increased compared to the case without axial injection, but the flashback behavior becomes worse due to the decrease of mixing quality. The adverse effect of the fuel rich zones (high flame velocities) on the flashback behavior due to insufficient radial distribution of the fuel is stronger in this case than the beneficial effect of the higher momentum on the axis. For higher axial fuel injection ratios the effect of the additional axial momentum outweighs the lack of mixing quality. However, the results for the fuel nozzle N2 show that this conclusion is only valid up to a certain fuel split. For very high axial momentum at 100% axial injection the flashback behavior becomes worse again. This is due to the fact that with higher axial fuel injection momentum the macroscopic mixing becomes better, resulting from the high shear between the fuel and airflow. This effect has already been shown in water channel experiments [1]. The increased fuel transport in radial direction has the consequence that more fuel reaches the wall region. Since the equivalence ratio on higher radii increases, laminar flame speeds s_l of up to 12 m/s are reached and the flame is able to enter the mixing section against the bulk flow, due to the the low axial velocities in this region [1] in the tests.

NO_x emissions of the different configurations were measured at a thermal power of 200kW and an adiabatic flame temperature of approx. 1800K. The residence time between burner exit and the sampling probe was 70 ms. In Figure 11 the line-of-sight integrated time-averaged OH*-chemiluminescence distributions (top) and the Abel-deconvoluted images (bottom) are shown with the corresponding NO_x (@ 15% O_2) values for injector N1.

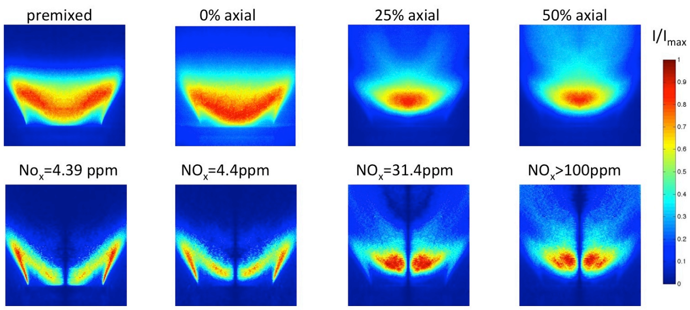

FIG. 11: NO_x-emissions and OH*-chemiluminescence

The externally premixed configuration and the TE injection (0% axial) exhibit the same flame shape and also the NO_x values are very similar, a clear indication that the trailing edge injection delivers very good mixing. When looking at the injection scenarios with axial injection one can see a change of the heat release distribution. As expected from the water channel tests [1] the flame moves downstream. This effect becomes stronger when the axial injection ratio increases. One can also see that the position of the RCZ is shifted and that the heat release becomes concentrated in the center of the RCZ due to worse radial mixing. The Abel-deconvoluted pictures also show that the flame stabilization in the outer shear layer decreases with increasing axial injection. This indicates that for the axial injection with pure hydrogen the fuel is not properly distributed over the complete outlet area, but is concentrated near the center. Consequently, NO_x values increase sharply. However, with undiluted hydrogen the potential of the injection of axial fuel momentum is very limited, whereas with MBTU or LBTU syngases much higher axial momentum is available. As previously demonstrated in the water channel tests [1] substantially better mixing and lower emissions can be expected for such fuels.

Flashback limits of trailing edge (TE) injection: Since the TE-injection showed NO_x emissions almost at the level of the externally premixed case, a detailed investigation of the flashback limits of this configuration was made. The operational windows of the configuration with and without diffuser are compared to each other and also to models and data from the literature.

For the **configuration without diffuser** it was shown that the flashback is initiated by flame propagation on the axis like previously observed in CIVB studies. For this reason, the instability data was compared to the model of Konle [8]. This model is based on the comparison of the chemical and turbulent timescales and allows to scale the flashback behavior of a burner to other operating conditions by measuring only one reference point. The Konle model was introduced for moderate turbulence in the center of the swirling flow, which is also characteristic for the flames in the experiments presented here. The model can be reduced to the Equation 1 for a specific burner, fuel, temperature and pressure.

$$\frac{\overline{u}}{s_l} = C_b \tag{1}$$

According to the model C_b is constant for all flashback points. Figure 12 shows the comparison of the data with the model, but also a comparison of the externally premixed and TE-injection. Interestingly, the configuration with TE-injection is slightly more

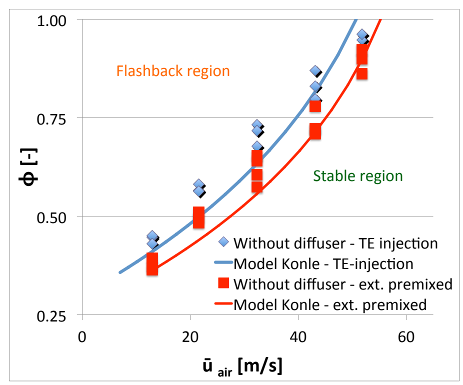

FIG. 12: Flashback limits and Konle model

flashback resistant than the perfectly premixed case. This can be explained by the distribution of the fuel holes along the trailing edge in the swirler. The LIF-mixing studies reported in [1] show that the core of the flow is 11% leaner compared with the perfectly premixed configuration. This leaner core leads to lower flame velocities in the center and therefore to better resistance against flame propagation. In addition, the predictions of the Konle model are plotted. When looking at the premix data (red line) the model fits the measured data almost perfectly. For the TE-injection data the Konle model was adapted by using the C_b of the premixed data at $\bar{u}$=43m/s and by calculating the blue curve with the lower equivalence ratio (-11%). The good fit to the data validates the assumption that the leaner vortex core is responsible for the better flashback limits achieved with TE-injection.

Since solely wall flashback was observed for the **configuration with diffuser**, the flashback limits of this configuration were compared to tube burner WBLF data from Kithrin [9]. For this purpose the critical gradient was calculated using the wall friction concept of Blasius for fully developed turbulent flows [10] at the measured flashback points according to:

$$g_{crit} = 0.03955 \cdot \bar{u}^{\frac{7}{4}} \cdot D^{-\frac{1}{4}} \cdot \eta^{-\frac{3}{4}} \cdot \rho^{\frac{3}{4}}. \tag{2}$$

Since the data of Kithrin was measured at atmospheric conditions, a temperature correction had to be applied to the measured data to map the data to ambient temperature. The only available correction was proposed by Fine [11]:

$$g^*_{crit} = g_{crit} \cdot \left(\frac{T_{amb}}{T_{preheat}}\right)^{1.52} \tag{3}$$

In Figure 13 the red points characterize the measured data and

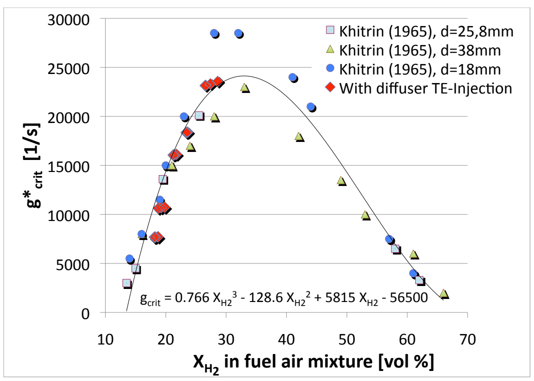

FIG. 13: Critical gradient comparison

the others the tube burner data from literature. It is shown that even though the proposed burner produces a rotating flow that is not fully developed and higher Reynolds numbers compared to the tube burners tested by Kithrin, the literature data predicts the wall flashback limits of the burner with diffuser very well.

To be able to compare the boundary layer flashback data to the CIVB data, a trend line was generated on the basis of all available WBLF data. A polynomial function of third order was used to describe the influence of the hydrogen content in the hydrogen air mixture on the critical wall velocity gradient (see Figure 13). This function and Equations 2 and 3 lead to a curve (see red curve in Figure 14) showing the equivalence ratio ϕ at the flashback limit with respect to the burner exit bulk velocity $\bar{u}_{air}$.

In Figure 14 the premixed data as well as the data from the TE-injection are plotted. The premixed configuration is more flashback resistant in this case. Due to the scaling of the ordinate the effect appears smaller compared to the difference observed for CIVB initiated flashback (Figure 12), but in fact the differences are similar. The root cause for the observed differences is again the radial fuel profile, but with opposite consequence: The

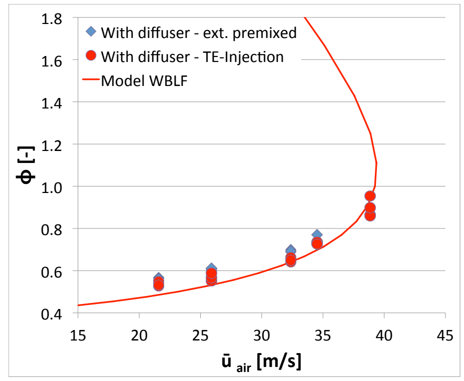

FIG. 14: Measured WBLF limits compared to applied model

leaner core of the flow automatically leads to a fuel richer wall region, to higher flame velocities there and to a slight deterioration of the resistance against WBLF.

Comparing now the configurations with and without diffuser (Figure 15) one can see that the two flashback limits are very close to one another. This result is not that astonishing since for the configuration without diffuser the flashback starts with flame propagation in the center of the flow and transits to wall flashback.

In Figure 15 also the turbulent flame speed $s_t = s_l + u'$ is plotted in green for an assumed turbulence level of 10%. The laminar flame speed was extracted from Chemkin using the GRI 3.0 mechanism. The green line shows that the turbulent flame speed in the experiments with low flow bulk velocities cannot be considered small with respect to the local flow velocity. As the consequence, the low flow velocity allows radial flame propagation in a steep angle against the axial flow direction. This also indicates that the transition from flame propagation on the axis to wall flashback, observed in the burner without diffuser, can be due to turbulent flame propagation.

At typical full load burner equivalence ratios of $\phi \approx 0.5$ the bulk flow velocity required for provoking flashback at atmospheric pressure are by a factor 4 lower than typical flow speeds

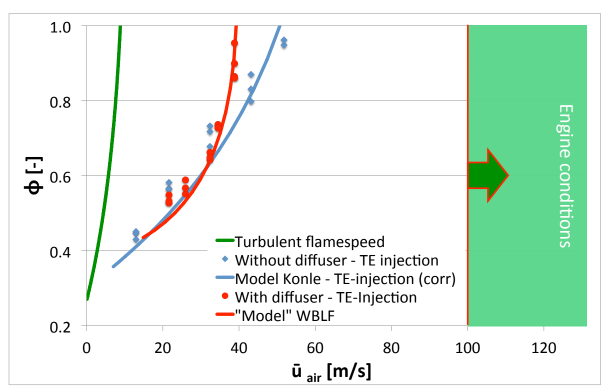

FIG. 15: Comparison of flashback limits

in premix burners of gas turbines but the influence of pressure must be additionally considered before safety margins can be derived.

Combustion experiments at elevated pressure

In the pressurized tests the **configuration with diffuser** was used, which exhibited WBLF in the atmospheric tests. Stability maps were measured, the flame shape was determined on the basis of the OH*-chemiluminescence to get more information about the flame contour under elevated pressure and also ionization probes were applied for the detection of reaction near the mixing tube walls. Insofar as no other figures will be given, the air preheat temperature was 150°C and the pressure drop over the burner of $\Delta p_{Br} = 1\%$.

Externally premixed CH_4: At first CH_4 combustion in the externally premixed mode was investigated in a pressure range from 1bar to 7bar. For the burner geometry no flashback could be detected for natural gas combustion and the LBO limit was found at an adiabatic flame temperature of approx. 1700K. This result confirms the very stable behavior of the burner for CH_4 shown earlier in atmospheric combustion experiments [1]. As expected, flashback could also not be provoked in additional tests with higher pressure drop over the burner.

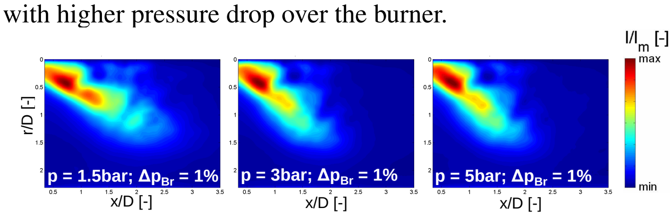

FIG. 16: OH*-chemiluminescence, influence of pressure on flame shape, externally premixed case, $\phi = 0.7$

The flame front gets longer due to the decreasing combustion temperature and the lower reaction rate for lower equivalence ratios [13]. The tip of the flame was found to reside inside of the diffuser and the angle of the outer envelope of the v-shaped flame is slightly reduced with decreasing equivalence ratio. In the measured range the pressure has nearly no effect on the flame contour (see Figure 16).

For a pressure of p=1.5bar and p=3bar (Figure 17) the OH*-signals of a stoichiometric and a leaner flame with three different pressure drop ratios (Δp_{Br}= 1%, 2% and 3%) were measured (Figure 17). It was found that the pressure drop over the burner has an effect on the flame contour. Increasing the pressure drop leads to a moderate increase of the flame length. These results of the HP-tests are consistent with the trends observed in the atmospheric combustion tests.

Externally premixed CH_4-H_2 mixtures and H_2: For comparison of the downscaled burner in the high pressure test rig with the bigger version tested in the atmospheric combustion test rig a first set of experiments was made at p=1,5bar, which is the

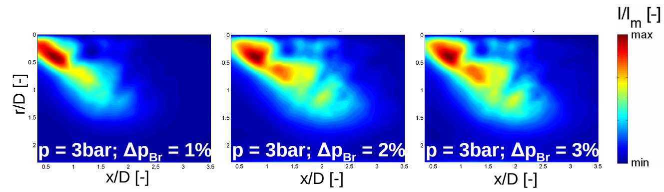

FIG. 17: OH*-chemiluminescence, influence of pressure drop on flame shape, externally premixed case, $\phi = 0.7$

minimum pressure required for proper operation of the high pressure test rig. Pressure drops of $\Delta p_{Br} = 1\%$ and $\Delta p_{Br} = 3\%$ were investigated. In Figure 18 the flashback (blue filled rhombuses) and LBO limits (blue empty rhombuses) limits are shown. As expected, the LBO is shifted towards lower equivalence ratios by increasing the hydrogen fuel fraction. Below a H_2 fuel fraction of approx. 60% no flashback could be provoked even at stoichiometric conditions. For operation points with higher hydrogen fuel fractions the critical ϕ for flashback decreases down to 0.56 for 100% H_2. An increase of pressure drop has only a minor positive influence on the flashback limit and it has a minor negative effect on the LBO limit (not shown in Figure 18).

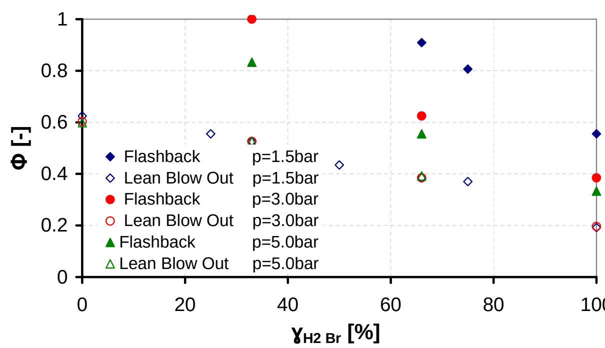

FIG. 18: HP test rig stability map, influence of hydrogen content on flashback and LBO, externally premixed case

The stability limits of the downscaled burner under elevated pressure (p = 3bar and p = 5bar) are also shown in Figure 18. To save hydrogen, cost and test time, only configurations with a volume fraction of 33%, 66% and 100% hydrogen were measured at higher pressure. The results show that the lean blow out limits are almost not affected by pressure in this range. However, the flashback limit strongly deteriorates with increasing pressure. Even for small hydrogen volume fractions of 33% flashback occurs at $\phi_{p=3bar} = 1.0$ and $\phi_{p=5bar} = 0.83$, respectively. For pure hydrogen the value for the critical ϕ lies at approx. 0.33.

In Figure 19 the flame contours are shown either for ϕ=1.0 or the equivalence ratio shortly before flashback, respectively. For these cases the chemiluminescence images showed clearly that with increasing hydrogen content the flame becomes substantially shorter, indicating a significant influence of the fuel reactivity on the turbulent flame speed. The same effect was seen in atmospheric combustion tests before [1]. The influence of the

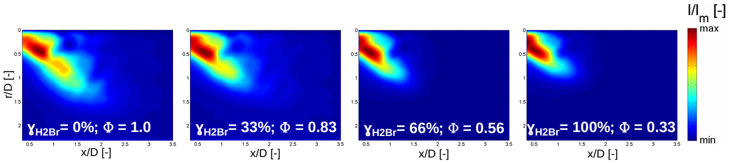

FIG. 19: OH*-chemiluminescence, flame shape for stoichiometic conditions or before flashback, respectively, externally premixed case, p = 5bar

pressure is as marginal as before and the changes observed when increasing the pressure drop are qualitatively the same as for the combustion of CH_4 (natural gas).

Axial H_2 injection: The influence of axial injection of H_2 on the operational window of the burner is shown in Figure 20. In these experiments the CH_4 was supplied externally premixed and enters the burner together with the combustion air through the four slots and the annular gap around the axial injector at the apex of the conical swirler. The hydrogen was injected through the axial nozzle placed in the center of the axial inlet. For the same reasons as mentioned above flashback limits were only measured for 33%, 66% and 100% hydrogen and the LBO limits only once for 1.5 bar pressure.

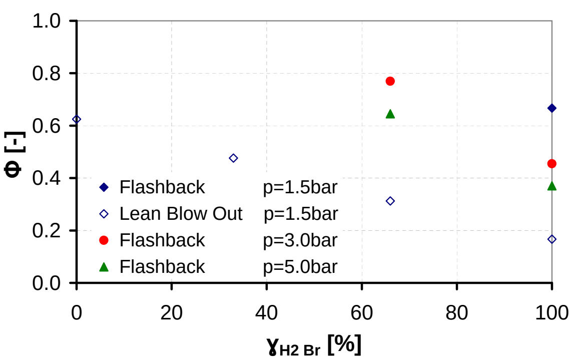

FIG. 20: HP test rig stability map, influence of axial H_2 injection on flashback and LBO

The comparison with the externally premixed experiments (Figure 18) shows that the stable operation window is increased. Flashback limits are moved towards higher and LBO limits towards lower equivalence ratios. For 33% H_2 fuel fraction no flashback could be provoked anymore. For higher hydrogen concentration the flashback limit improves by approx. 10% in terms of equivalence ratio compared to the cases without axial H_2 injection and external premixing of all fuel.

Compared to the externally premixed experiments significant differences in the flame contour were observed. Due to the higher axial momentum with increasing H_2 fuel fraction the flame shape changes significantly towards a turbulent jet flame for 100% H_2. The flame becomes longer and its opening angle decreases with increasing H_2 fuel fraction (Figure 21). As shown previously [1] in water channel experiments with different mo-

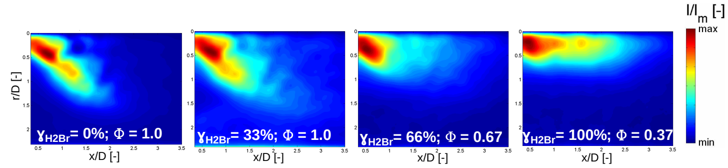

FIG. 21: HP Test Rig: OH* Chemiluminescence Images, Axial H_2 Injection, p = 5bar

mentum density ratios at the axial inlet, the changing flame shape results from the shift of the recirculation zone downstream ultimately resulting in the generation of a swirling jet without vortex breakdown for sufficiently large axial fuel momentum. By comparing the water channel test results with the high pressure experiments using 100% H_2 (Figure 21) at equal fuel momentum it can be concluded that increasing H_2 leads to the desirable transition from vortex breakdown flame stabilization to the flame stabilization pattern observed in turbulent jets with swirl.

The ionization measurements near the wall confirm that WBLF occurs in the high pressure test rig although the hydrogen has been injected axially on the axis in downstream direction. Comparing the flashback limits of the externally premixed configuration and the configuration with axial hydrogen injection, reveals that axial injection was not as efficient as desired for the configuration with diffuser that exhibits WBLF. However, axial injection is intended to stabilize the center of the flow, which is not the problematic region once the transition of the flame stabilization to the region near the diffuser walls has occurred. Unfortunately, axial injection does not lead to steeper wall gradients, which would be beneficial for the resistance against WBLF. It has been shown [1] that for axial H_2 injection leaner conditions exist on higher radii and a fuel overshoot is generated on the axis of the burner. This indicates that observed positive effect of axial fuel injection on the flashback limits stems primarily from the lower equivalence ratio near the mixing tube wall. As desired, the vortex core region of the flow is stabilized by the axial momentum introduced with the fuel, because flame propagation near the axis is not observed despite the large equivalence ratio on the axis.

In summary, all findings from the tests under elevated pressure concerning the operation window, flame contour and flashback mechanism are consistent with the atmospheric combustion experiments. This is the prerequisite for the quantitative analysis of the effect of pressure on WBLF presented in the next section.

Influence of pressure on the flashback limits:

On the basis of the observed flashback type under atmospheric conditions and elevated pressure the conclusion can be drawn that WBLF is the most critical issue. In the analysis the flashback limits for the externally premixed configurations with diffuser and for hydrogen combustion will be employed.

For this purpose the critical gradient was calculated like in the atmospheric experiments before (Equation 2) and the temperature correction introduced before was applied (Equation 3). This procedure leads to the important result that the critical gradients required for avoiding WBLF steeply rise with pressure. To account for the pressure effect an additional correlation was applied, which was also proposed by Fine [14].

$$g_{crit}^{**} = g_{crit}^{*} \left(\frac{p_{amb}}{p_{exp}} \right)^{1.35} \tag{4}$$

This correlation predicts that the critical gradient will rise by a factor of almost 60 when the pressure is increased from atmospheric testing conditions to typical engine pressures. Figure 22 shows the result when Equation 4 is applied to the data obtained in the high pressure test rig.

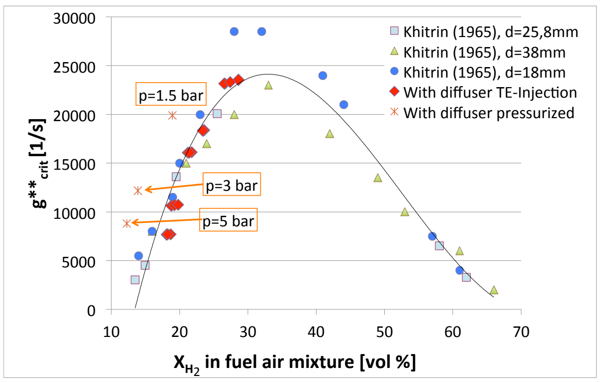

FIG. 22: Critical gradient comparison

For the high pressure experiments the temperature and pressure corrections led to much higher critical gradients than the atmospheric data. The results indicate that pressure correction did neither deliver precise nor conservative results for the mapping of the atmospheric laboratory data to the data acquired at elevated pressure employing the downscaled burner. For engine pressure an even more problematic situation must be expected.

Moreover, Eichler and Baumgartner show in [15] that the critical gradient required to avoid flame propagation in the burner is almost one order of magnitude higher than the gradients needed for flame penetration from the combustor into the burner along the wall boundary layers, which is investigated in this study. As the consequence, providing enough recovery potential of syngas burners after flashback is more challenging than flashback prevention.

In summary, the present study and the results presented in [15] demonstrate that safe engine operation is difficult to achieve even if the burner shows excellent WBLF flashback resistance in atmospheric tests. There is evidence that sufficient safety against WBLF may require a reduction of the fuel concentration near the burner walls towards very low equivalence ratios.

Conclusions and Outlook

A detailed analysis of the nature of flashback for the combustion of hydrogen and mixtures of hydrogen and natural gas in a swirl burner with conical mixing tube was provided. Configurations with and without diffuser attached to the mixing tube and three types of fuel injection methods were tested and the influence of pressure was also investigated.

- For natural gas flashback could not be provoked at atmospheric pressure even at very low flow velocities and stoichiometric conditions.
- For hydrogen flashback was observed at atmospheric pressure and stoichiometric conditions only if the flow velocities were reduced to less than 50% of the burner bulk velocities typical for engine operation. For lean mixtures an even larger reduction of the velocity was required for achieving flashback.
- For premixed hydrogen different flashback types were observed depending on the flow conditions at the burner exit: In the case with diffuser the flame propagates in the wall boundary layer. Without diffuser three consecutive phases were observed starting with flame propagation on the axis and ending again with flame propagation in the wall boundary layer. The flashback limits for both configurations lie very close to each other.
- Increasing the pressure leads to a deterioration of flashback safety. At engine pressure avoiding boundary layer flashback will be very difficult without reduction of the equivalence ratio near the burner walls.
- Models and correlations available from literature showed to be applicable to the flashback limit data for the premixed combustion of hydrogen at atmospheric conditions.
- Trailing edge injection of hydrogen in the swirler leads to low emissions as well as a robust stability behavior at atmospheric pressure.
- Axial injection of undiluted hydrogen leads to a steep rise of emissions, but only to a rather moderate further improvement of the flashback limits compared to the limits observed for trailing edge injection.

Since the combustion of undiluted hydrogen is technically less relevant than the combustion of syngas with inert components the study will be extended to diluted fuels in the future. These investigations will be focussed on the potential of tailoring the flow field with axial injection of such fuels, which offer a much higher potential for providing axial momentum than undiluted hydrogen and a better tradeoff with emissions.

ACKNOWLEDGMENT

The investigations were conducted as part of the joint research programme COORETEC-turbo in the frame of AG Turbo. The work was supported by the Bundesministerium für

Wirtschaft und Technologie (BMWi) as per resolution of the German Federal Parliament. The authors gratefully acknowledge AG Turbo and Alstom Power for their support and permission to publish this paper. The responsibility for the content lies solely with its authors.

REFERENCES

[1] J. Sangl, C. Mayer, T. Sattelmayer, *Dynamik adaptation of aerodynamic flame stabilization of a premix swirl burner to fuel reactivity using fuel momentum*, June 2010, No. GT2010-22340, in: Proceedings of ASME Turbo Expo 2010, Glasgow, Scotland, accepted for publication in: Journal of Engineering for Gas Turbines and Power

[2] J. Fritz, M. Kröner, T. Sattelmayer, *Flashback in a Swirl Burner with Cylindrical Premixing Zone*, 2004, Journal of Engineering for Gas Turbines and Power, Vol. 126, No. 2, pp. 276-283

[3] M. Kröner, J. Fritz, T. Sattelmayer, 2003, *Flashback Limits for Combustion Induced Vortex Breakdown in a Swirl Burner*, Journal of Engineering for Gas Turbines and Power, Vol. 125, No. 3, pp. 693-700

[4] V. Dibrinski, A. Ossadtchi, V. Mandelshtam, H. Reisler, *Reconstruction of Able-Transformable Images: The Basis-St Expansion Abel Transform Method*, 2002, Rev. SCI. Instrum., Vol. 73, No. 7, pp. 2635-2642

[5] E. Freitag, *On the measurement and Modelling of Flame Transfer Functions at Elevated Pressure*, April 2009, Ph. D. Thesis, Technische Universität München

[6] E. Freitag, H. Konle, M. Lauer, C. Hirsch, T. Sattelmayer, *Pressure Influence on the Flame Transfer Function of a premixed swirling Flame*, May 2006, No. GT2006-60540, in: Proceedings of ASME Turbo Expo 2006, Barcelona, Spain

[7] H. Zu, J.R. Laker, E. Mastorakos, C. Vafidis, H.M. Xu, *The development and application of a fast-response DC-coupled flame ionization current sensor*, 1993, Experiments in Fluids, Vol. 14, pp. 316-320

[8] M. Konle, T. Sattelmayer, *Time scale model for the prediction of the onset of flame flashback driven by Combustion Induced Vortex Breakdown (CIVB)*, 2010, Journal of Engineering for Gas Turbines and Power, Vol. 132, No. 4, pp. 041503

[9] L.N. Khitrin, P. B., *Peculiarities of laminar- and turbulent-flame flashbacks*, 1965, 10th Symposium (Int.) on Combustion , pp. 1285-1291

[10] H. Schlichting, *Grenzschicht-Theorie*, 1982, Verlag G. Braun

[11] B. Fine, *Effect of Initial Temperature on Flash Back of laminar and Turbulent Burner Flames.*, 1959, Industrial and Engineering Chemistry, Vol. 51, No. 4, pp. 564-566.

[12] S. Burmberger, *Optimierung der aerodynamischen Flammenstabilisierung für brennstoffflexible vorgemischte Gasturbinenbrenner*, March 2009, Ph. D. Thesis, Technische Universität München

[13] P. Siewert, *Flame front characteristics of turbulent lean premixed methane/air flames at high pressure*, 2006, Ph. D. Thesis, ETH Zürich,

[14] B. Fine, *The Flashback of Laminar and Turbulent Burner Flames at Reduced Pressure.*, 1958, Combustion and Flame, Vol. 2, No. 3, pp. 253-266

[15] C. Eichler, G. Baumgartner, T. Sattelmayer, *Experimenteal Investigation of Turbulent Boundary Layer Flashback Limits for Premixed Hydrogen-Air Flames Confined in Ducts*, June 2011, No. GT2010-45362, in: Proceedings of ASME Turbo Expo 2011, Vancouver, Canada, accepted for publication in: Journal of Engineering for Gas Turbines and Power